Mon. Not. R. Astron. Soc. **000**, 1–15 (2002) Printed 2 February 2008 (MN LATEX style file v2.2)

The Morphology-Density Relation in the SDSS

Tomotsugu Goto[1,2⋆], Chisato Yamauchi[3], Yutaka Fujita[3], Sadanori Okamura[2], Maki Sekiguchi[1], Ian Smail[4], Mariangela Bernardi,[5] and Percy L. Gomez[5]
[1] *Institute for Cosmic Ray Research, University of Tokyo, Kashiwanoha, Kashiwa, Chiba 277-0882, Japan*
[2] *Department of Astronomy, Graduate School of Science, The University of Tokyo, Hongo 7-3-1, Bunkyo-ku, Tokyo 113-0033, Japan*
[3] *National Astronomical Observatory, 2-21-1 Osawa, Mitaka, Tokyo 181-8588,Japan*
[4] *Department of Physics, University of Durham, South Road, Durham DH1 3LE, UK*
[5] *Department of Physics, Carnegie Mellon University, 5000 Forbes Avenue, Pittsburgh, PA 15213, USA*

2 February 2008

ABSTRACT

We have studied the morphology-density relation and morphology–cluster-centric-radius relation using a volume limited sample ($0.05< z <0.1$, $Mr^* < -20.5$) of the Sloan Digital Sky Survey (SDSS) data. Major improvements compared with previous work are; (i) automated galaxy morphology classification capable to separate galaxies into four types, (ii) three dimensional local galaxy density estimation, (iii) the extension of the morphology-density relation into the field region. We found that the morphology-density and morphology–cluster-centric-radius relation in the SDSS data for both of our automated morphological classifiers, *Cin* and *Tauto*, as fractions of early-type galaxies increase and late-type galaxies decrease toward increasing local galaxy density. In addition, we found there are two characteristic changes in both the morphology-density and the morphology-radius relations, suggesting two different mechanisms are responsible for the relations. In the sparsest regions (below 1 Mpc^{-2} or outside of 1 virial radius), both relations become less noticeable, suggesting the responsible physical mechanisms for galaxy morphological change require denser environment. In the intermediate density regions (density between 1 and 6 Mpc^{-2} or virial radius between 0.3 and 1), intermediate-type fractions increase toward denser regions, whereas late-disc fractions decrease. Considering the median size of intermediate-type galaxies are smaller than that of late-disc galaxies, we propose that the mechanism is likely to stop star formation in late-disc galaxies, eventually turning them into intermediate-type galaxies after their outer discs and spiral arms become invisible as stars die. For example, ram-pressure stripping is one of the candidate mechanisms. In the densest regions (above 6 Mpc^{-2} or inside of 0.3 virial radius), intermediate-type fractions decrease radically and early-type fractions increase in turn. This is a contrasting result to that in intermediate regions and it suggests that yet another mechanism is more responsible for the morphological change in these regions.

We also compared the morphology-density relation from the SDSS ($0.01< z <0.054$) with that of the MORPHS data ($z \sim 0.5$). Two relations lie on top of each other, suggesting that the morphology-density relation was already established at $z \sim 0.5$ as is in the present universe. A slight sign of an excess elliptical/S0 fraction in the SDSS data in dense regions might be suggesting the additional formation of elliptical/S0 galaxies in the cluster core regions between $z = 0.5$ and $z = 0.05$.

Key words: galaxies: clusters: general

1 INTRODUCTION

Morphological types of galaxies are one of the most basic properties and thus have been studied since the beginning of the extragalactic astronomy (e.g., Roberts & Haynes 1994).

⋆ E-mail: yohnis@icrr.u-tokyo.ac.jp

However, it is still not very well understood where this diversity stems from. The existence of a correlation between galaxy morphology and local environment is a remarkable feature of galaxy population. Dressler (1980) studied 55 nearby galaxy clusters and found that fractions of elliptical galaxies increase and that of spiral galaxies decrease with increasing local galaxy density in all clusters. The discovery left a great impact on astronomical community since it indicates that physical mechanisms that depend on environment of each galaxy mainly affect the final configuration of stellar component. Further observational constraints on the formation and evolution of galaxies were obtained by extending the analysis of the morphology-density relation to group of galaxies in the general field. Postman & Geller (1984) extended morphology study to groups using the data from the CfA Redshift Survey (Huchra et al. 1983). The relation was completely consistent with Dressler (1980). At low densities, population fractions seemed to be independent of density below galaxy density $\sim$5 Mpc^{-3}. At high density, the elliptical fraction increased steeply above $\sim$3000 galaxies Mpc^{-3}. Therefore, they proposed the morphology-density relation have three distinct regions or two breaks which are related to the timescale of different physical mechanisms acting upon the galaxy populations. The morphology-density relation is also observed in X-ray selected poor groups. Tran et al. (2001) studied six nearby X-ray detected, poor groups and found that the fraction of bulge-dominated galaxies in groups decreases with increasing radius, similar to the morphology-density relations in clusters. Helsdon & Ponman (2002) observed the morphology-density relation in groups and found that X-ray bright groups have a lower spiral fraction. The opposite results on groups came from Whitmore et al. (1995). They analyzed the morphology-density relation in groups of galaxies by carefully removing cluster galaxies from their analysis and found that the relation is very weak or non-existent in groups.

It is important to note that Whitmore et al. (1991,1993) re-analyzed the 55 nearby clusters (Dressler 1980) and argued that the morphology-density relation reflects a more fundamental morphology-radius relation; the correlation between morphology and cluster centric radius seems tighter than the morphology-density relation. Although this assertion is still controversial, it may have a significant implication for underlying physical mechanisms.

Later the relation between morphology and density was traced back to higher redshift. Dressler et al. (1997) studied 10 high redshift clusters at z $\sim$0.5 and found that the morphology-density relation is strong for centrally concentrated clusters. However, the relation was nearly absent for less concentrated or irregular clusters. They also found that S0 fractions are much smaller than in nearby clusters, suggesting that S0 galaxies are created fairly recently ($z \leqslant$0.5). At z = 0.4, Treu et al. (2003) found that the fraction of early-type galaxies declines steeply from the cluster center to 1 Mpc radius using the cluster Cl0024+16. Fasano et al. (2000) studied nine clusters at intermediate redshift ($0.1 \leqslant z \leqslant 0.25$) and compared them with local (Dressler 1980) and high redshift clusters (Dressler et al. 1997). They found that morphology-density relation in high elliptical concentration clusters, but not in low elliptical concentration clusters. The finding is consistent with the results of Dressler et al. (1997). Considering that low redshift clusters have morphology-density relation regardless of the concentration of clusters, they suggested that spiral to S0 transition happened fairly recently (last 1-2 Gyr). They also plotted morphological fraction as a function of redshift and found that S0 fraction decreases with increasing redshift, whereas spiral fraction increases with redshift.

Hashimoto et al. (1999) used data from Las Campanas Redshift Survey (LCRS; Shectman et al. 1996) to study the concentration-density relation. They found that the ratio of high and low concentrated galaxies decreases smoothly with decreasing density. Dominguez et al. (2001) analyzed nearby clusters with X-ray and found that mechanisms of global nature (X-ray mass density) dominate in high density environments, namely the virialized regions of clusters, while local galaxy density is the relevant parameter in the outskirts where the influence of cluster as a whole is relatively small compared to local effects. Dominguez et al. (2002) studied groups in 2dF Galaxy Group Catalog using PCA analysis of spectra as a galaxy classification and local galaxy density from redshift space as a measure of galaxy environment. They found that both morphology-density relation and morphology-group-centric radius relation is clearly seen in high mass ($Mv \geqslant 10^{13.5} M_{\odot}$) groups, but neither relation holds true for low mass ($Mv < 10^{13.5} M_{\odot}$) groups. These three studies made innovative step in terms of an analysis method, using automated morphological classification and three dimensional density estimation.

Various physical mechanisms have been proposed to explain the morphology-density relation. Possible causes include ram-pressure stripping of gas (Gunn & Gott 1972; Farouki & Shapiro 1980; Kent 1981; Fujita & Nagashima 1999; Abadi, Moore & Bower 1999; Quilis, Moore & Bower 2000), galaxy harassment via high speed impulsive encounters (Moore et al. 1996, 1999; Fujita 1998), cluster tidal forces (Byrd & Valtonen 1990; Valluri 1993; Fujita 1998) which distort galaxies as they come close to the centre, interaction/merging of galaxies (Icke 1985; Lavery & Henry 1988, Mamon 1992; Makino & Hut 1997; Bekki 1998; Finoguenov et al. 2003a), and removal & consumption of the gas due to the cluster environment (Larson, Tinsley & Caldwell 1980; Bekki et al. 2002; Finoguenov et al. 2003b). Shioya et al. (2002) showed that the truncation of star formation can explain the decrease of S0 with increasing redshift. Although these processes are all plausible, the effects provided by initial condition on galaxy formation could be also important. Since field galaxies have different population ratio compared with clusters (Goto et al. 2002a), a change in infalling rate of field galaxies into clusters affects population ratio of various galaxy types (Kodama et al. 2001). Unfortunately, there exists little evidence demonstrating that any one of these processes is actually responsible for driving galaxy evolution. Most of these processes act over an extended period of time, while observations at a certain redshift cannot easily provide the detailed information that is needed to elucidate subtle and complicated processes.

To extract useful information from observational data, it is necessary to have detailed theoretical predictions. In recent years, due to the progress of computer technologies, it is becoming possible to simulate the morphology-density relations by combining semi-analytic modeling with N-body simulations of cluster formation. Okamoto & Nagashima (2001) simulated the morphology-density relation

using a merger-driven bulge formation model. They found that early-type fractions are well re-produced, but there remained a discrepancy on intermediate-type fractions. Diaferio et al. (2001) also assumed that the morphologies of cluster galaxies are determined solely by their merging histories in the simulation. They used bulge-to-disc ratio to classify galaxy types and compared the cluster-centric radial distribution with those derived from CNOC1 sample (Yee,Ellingson, & Carlberg 1996). They found excellent agreement for bulge dominated galaxies, but simulated clusters contained too few galaxies of intermediate bulge-to-disc ratio. Springel et al. (2001) used a phenomenological simulation to predict the morphology-radius relation and compared it with Whitmore et al.(1993). Their morphological modeling is based on the merging history of galaxies. They found an excellent agreement with early-type galaxy fractions, and some deficiency of intermediate-type galaxies in the core of the cluster. Benson et al. (2001) combined their N-body simulation with a semi-analytic model (Cole et al. 2000) to trace the time evolution of the morphology-density relation. Interestingly, they found that a strong morphology-density relation was well established at z =1. The relation was qualitatively similar to that at z =0. E/S0 galaxies are treated as one population in their simulation. Three of above simulations suggest that (i) early-type fractions are consistent with the merging origin; (ii) however the deficit of intermediate-type galaxies shows that processes other than major-merger might be important for intermediate-type creation. Therefore, more than one mechanism might be required to fully explain the morphology-density relation. These suggestions might be consistent with observational results from Dominguez et al. (2001), who found two different key parameters in cluster centre and outskirts separately.

In the previous analysis of the morphology-density relation from observations, there have been two major difficulties; eye-based morphological classification and the density estimate from two-dimensional imaging data. Although it is an excellent tool to classify galaxies, manual selection could potentially have unknown biases (see Lahav et al. 1995; Fabricant et al. 2000). A machine based, automated classification would better control biases and would allow a reliable determination of the completeness and false positive rate. Measuring local galaxy density from imaging data requires statistical background subtraction, which automatically invites relatively large uncertainty associated with itself. Furthermore the deeper imaging data , the bigger the correction. Therefore, three dimensional density determination from redshift data is preferred. With the advent of the Sloan Digital Sky Survey (SDSS; York et al. 2000), which is an imaging and spectroscopic survey of 10,000 deg^2 of the sky, we now have the opportunity to overcome these limitations. Several of the largest cluster catalog are compiled using the SDSS data (Annis et al. 1999; Kim et al. 2002; Goto et al. 2002b). The CCD imaging of the SDSS allows us to estimate morphologies of galaxies in an automated way (Yamauchi et al. 2003). Three dimensional density can be estimated from the redshift information (e.g., Hogg et al. 2003). Due to the large area coverage of the SDSS, we are able to probe the morphology-density relation from cluster core regions to the field region without combining multiple data sets with inhomogeneous characteristics. The purpose of this paper is as follows. We aim to confirm or disprove the morphology-density relation using the automated morphology and three dimensional density from the SDSS data. We also re-analyze the MORPHS data (z $\sim$0.5) using an automated morphology (Smail et al. 1997). By comparing them to the SDSS, we try to observe the evolution of the morphology-density relation. Final goal of our investigation is to shed some light on the origin of the morphology-density relation.

The paper is organized as follows: In Section 2, we describe the SDSS data. In Section 3, we explain automated morphological classifications and density estimation. In Section 4, we present the results from the SDSS and the MORPHS data. In Section 5, we discuss the possible caveats and underlying physical processes which determines galaxy morphology. In Section 6, we summarize our work and findings. The cosmological parameters adopted throughout this paper are H_0=75 km s^{-1} Mpc^{-1}, and (Ω_m,Ω_Λ,Ω_k)=(0.3,0.7,0.0).

2 THE SDSS DATA

The data we use to study the morphology-density relation are from the Sloan Digital Sky Survey Early Date Release (SDSS EDR; Stoughton et al. 2002), which covers $\sim$400 deg^2 of the sky (see Fukugita et al. 1996; Gunn et al. 1998; Lupton et al. 1999,2001,2002; York et al. 2000; Eisenstein et al. 2001; Hogg et al. 2001; Blanton et al. 2003a; Richards et al. 2002; Stoughton et al. 2002; Strauss et al. 2002; Smith et al. 2002; Pier et al. 2003 for more detail of the SDSS data.) The imaging part of the SDSS observes the sky in five optical bands (u, g, r, i, and z; Fukugita et al. 1996). Since the SDSS photometric system is not yet finalized, we refer to the SDSS photometry presented here as u^*, g^*, r^*, i^* and z^*. The technical aspects of the SDSS camera are described in Gunn et al. (1998). The SDSS spectroscopic survey observes the spectra of essentially all galaxies brighter than r^*=17.77. The target galaxies are selected from imaging part of the survey (Strauss et al. 2002). The spectra are observed using a pair of double fiber-fed spectrographs obtaining 640 spectra per exposure of 45 minutes. The wavelength coverage of the spectrographs is continuous from about 3800 Å to 9200 Å, and the wavelength resolution, $\lambda/\delta\lambda$, is 1800. The fiber diameter is 0.2 mm (3″ on the sky). Adjacent fibers cannot be located closer than 55″ on the sky. The throughput of the spectrograph will be better than 25% over 4000 Å to 8000 Å excluding the loss due to the telescope and atmosphere. (See Eisenstein et al. 2001; Strauss et al. 2002 and Blanton et al. 2003a for more detail of the SDSS spectroscopic data).

We use galaxies in the redshift range 0.05$<$ z $<$0.1 with a redshift confidence of $\geqslant$ 0.7 (See Stoughton et al. 2002 for more details of the SDSS parameters). The galaxies are limited to $Mr^* < -20.5$, which gives us a volume limited sample with 7938 galaxies. We correct magnitudes for galactic extinction using reddening map of Schlegel, Finkbeiner & Davis (1998). We use k-correction given in Blanton et al. (2003b;v1_11) to calculate absolute magnitudes.

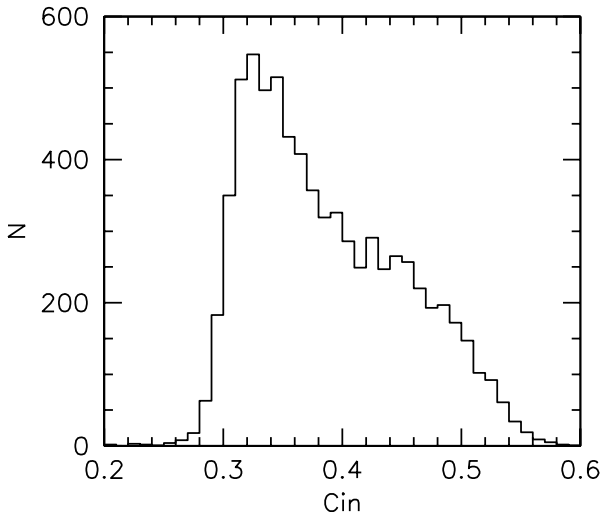

Figure 1. The distribution of *Cin* for the volume limited sample of 7938 galaxies.

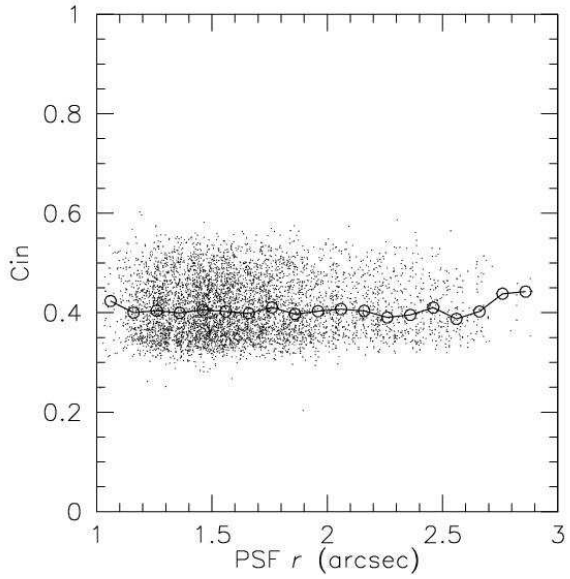

Figure 2. Seeing dependence of *Cin*. The solid lines show medians. 87% of our sample galaxies have seeing between 1.2 and 2 arcsec, where seeing dependence of *Cin* is negligible. The seeing is measure in r band.

3 ANALYSIS

3.1 Morphological Classification

We use two different ways of classifying galaxy morphologies. The first one is a concentration parameter *Cin*, which is defined as the ratio of Petrosian 50% light radius to Petrosian 90% light radius. We show the distribution of this *Cin* parameter in Figure 1. Shimasaku et al. (2001) and Strateva et al. (2001) showed that this *Cin* parameter correlates well with their eye-classified morphology (See Figure 10 of Shimasaku et al. 2001 and Figure 8 of Strateva et al. 2001). We regard galaxies with $Cin \geqslant 0.4$ as late-type galaxies and ones with $Cin < 0.4$ as early-type galaxies. The criterion of Cin=0.4 is more conservative for late-type galaxies. As shown by Shimasaku et al. (2001), Cin=0.4 provides late-type galaxy sample with little contamination and early-type galaxy sample with small contamination. The seeing dependence of *Cin* is presented in figure 2 for our volume limited sample galaxies. As is shown in figure 3, 87% of our sample galaxies have seeing between 1.2 and 2 arcsec where the dependence of *Cin* on seeing size is negligible.

The other classification uses morphological parameters measured by Yamauchi et al. (2003). We briefly summarize their morphological classification. Details on the method and various systematic tests including completeness and contamination study are given in Yamauchi et al. (2003)[1]. The classification method consists of two parts. In the first part, concentration index, *Ci*, is calculated as the ratio of the Petrosian 50% light radius and Petrosian 90% radius as is for *Cin* but the parameter is corrected for elongation of galaxies. The elongation correction prevent galaxies with low inclination (nearly edge-on galaxies) from being misclassified as early-type galaxies. In the second part, coarseness of galaxies, *Cn*, is calculated as the ratio of *residuals from the best fit of the galaxy radial profile* to *difference between the maximum and minimum values of the profile*. *Cn* is sensitive to arm structures of spiral galaxies, and thus larger for spiral galaxies with a clear arm structure than galaxies with a smooth radial profile such as ellipticals and S0s. This parameter, *Cn*, helps classifying late-type galaxies further into two types of galaxies. Finally, *Ci* and *Cn* are combined to be a final morphological parameter, *Tauto*. Both *Ci* and *Cn* are shifted so that their median values become 0.5, and

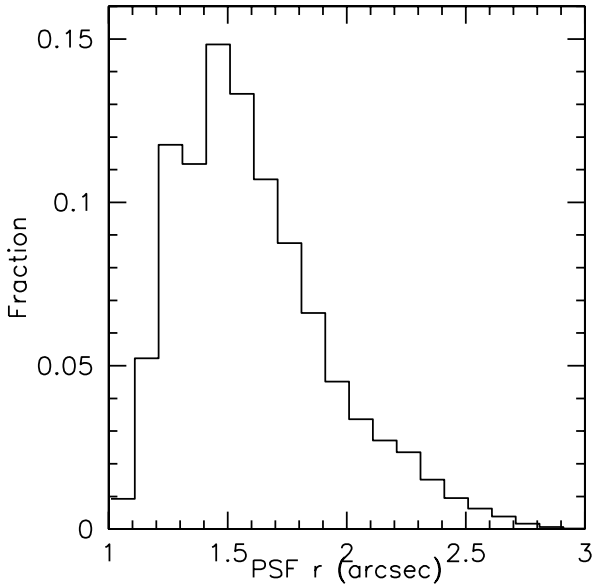

Figure 3. Distribution of seeing of the SDSS galaxies, measured in r band.

[1] Note that this work uses a preliminary version of *Tauto* parameter. The final parameter presented in Yamauchi et al. (2003) is expected to be improved further.

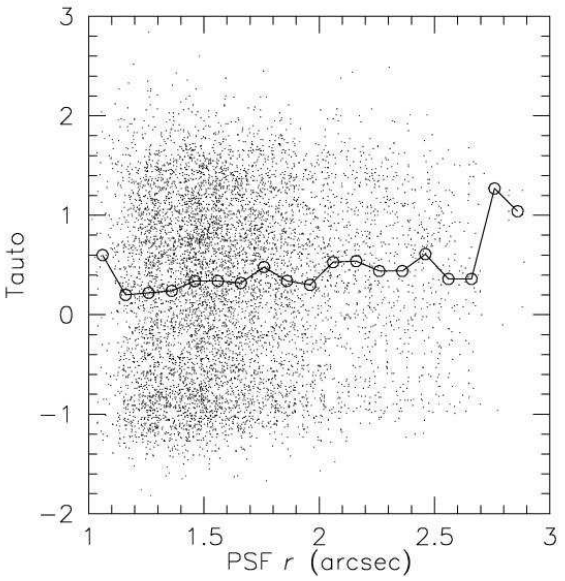

Figure 4. Seeing dependence of $Tauto$. The solid lines show medians of the distribution. $Tauto$ is essentially independent of seeing size between 1.2 and 2 arcsec, where 87% of our sample galaxies lie.

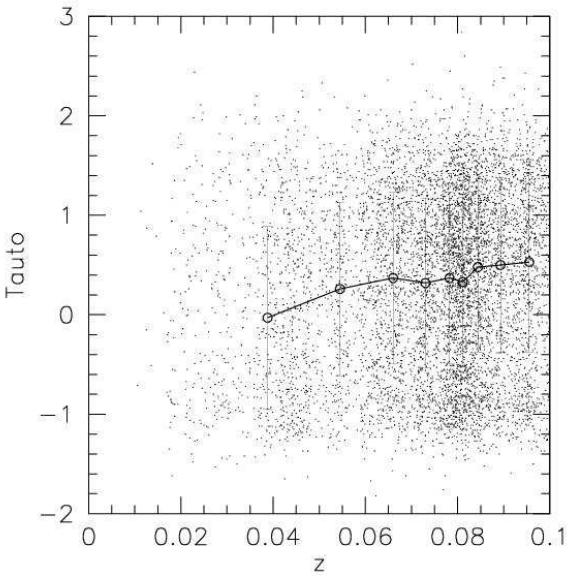

Figure 5. Redshift dependence of $Tauto$. The solid lines show medians of the distribution, which are consistent with constant throughout the redshift range we use ($0.05< z <0.1$). $Tauto$ shows some deviation at lower redshift ($z < 0.04$) since an apparent size of a galaxy on the sky radically increases at this low redshift.

then divided by its standard deviation to be combined to the final parameter to classify morphologies as follows.

$$Tauto = Ci(normalized) + Cn(normalized) \quad (1)$$

$Tauto$ shows better correlation with eye classified morphology than Cin, as shown in Yamauchi et al. (2003). The correlation coefficient with eye-morphology is 0.89. Based on the $Tauto$ parameter, we divide galaxies into four subsamples in this study. We regard galaxies with $Tauto >1.0$ as late-disc (LD) galaxies, $0.1< Tauto \leqslant 1.0$ as early-disc(ED), $-0.8 < Tauto \leqslant 0.1$ as intermediate-type (I, mostly S0s) and $Tauto < -0.8$ as early-type (E) galaxies. Among our sample galaxies, 549 galaxies have eye-classified morphologies (Shimasaku et al. 2001; Nakamura et al. 2003). In table 1, we quote completeness and contamination rate of these four types of galaxies classified by $Tauto$, using eye-classified morphology. Full discussion on contamination and completeness will be given in detail in Yamauchi et al. (2003). As shown in figure 4, the parameter is robust against seeing variance in our volume limited sample galaxies. In figure 5, we plot $Tauto$ against redshift. Medians are shown in the solid line. In our redshift range ($0.05< z <0.1$), $Tauto$ is essentially independent of redshift related bias.

In figure 6, Cin is plotted against $u-r$ colour. Strateva et al. (2001) pointed out that $u-r$=2.2 serves as a good galaxy type classifier as well. The distribution shows two peaks, one for elliptical galaxies at around $(u-r, Cin)$=(2.8,0.35), and one for spiral galaxies at around $(u-r, Cin)$=(2.0,0.45). Our criterion at Cin=0.4 is located right between these peaks and separates these two populations well. In figure 7, $Tauto$ is plotted against $u-r$ colour in four separate panels. Due to the inclination correction of $Tauto$, two populations degenerated in $u-r$ colour (around $u-r$=2.8) are now separated into early-type and early-disc galaxies, which is one of the major improvements of $Tauto$ against Cin. Overplotted points are galaxies classified by eye (Shimasaku et al. 2001; Nakamura et al. 2003). The upper left, upper right, lower left and lower right panels show elliptical, S0, early-spiral and late-spiral galaxies classified by eye, respectively. Compared with $Tauto$ criteria to separate the galaxies ($Tauto = -0.8$, 0.1 and 1.0), the figure suggests that our criteria separate galaxies reasonably well. The effect of inclination correction of $Tauto$ can be also seen in figure 8, where $Tauto$ is plotted against Cin. In addition to the nice correlation between the two parameters, there are galaxies with high $Tauto$ and low Cin values in the upper left of the figure. Most of these are edge-on galaxies correctly classified by $Tauto$ due to its inclination correction. In figure 9, we plot Hα EW for four types of galaxies classified with $Tauto$. Later type galaxies show higher Hα EWs, suggesting our galaxy classification criteria work well (see Kennicutt 1998).

3.2 Local Galaxy Density Measurements

We measure local galaxy density in the following way. For each galaxy, we measure a projected distance to the 5th nearest galaxy within $\pm$1000 km s^{-1} in redshift space among the volume limited sample ($0.05< z <0.1$, $Mr^* < -20.5$). The criterion for redshift space ($\pm$1000 km s^{-1}) is set to be generous to avoid galaxies with a large peculiar velocity slipping out of the density measurement, in other words, not to underestimate the density of cluster cores. Then, the number of galaxies ($N = 5$) within the distance is divided by the circular surface area with the radius of the distance to the 5th nearest galaxy. When the projected area touches the boundary of the data, we corrected the density by correcting the area to divide. Since we have redshift information for all of the sample galaxies, our density measurement is a pseudo-three dimensional density measurement and free

Table 1. Completeness and contamination rate of our four sample of galaxies classified by $Tauto$ are calculated using eye-classified morphology.

Type	Criteria	Completeness (%)	Contamination (%)
Early-type(E, mostly elliptical)	$Tauto \leqslant -0.8$	70.3	28.2
Intermediate(I, mostly S0)	$-0.8 \leqslant Tauto < 0.1$	56.4	56.5
Early Disc(ED, mostly Sa)	$0.1 \leqslant Tauto < 1.0$	53.1	24.1
Late Disc (LD, mostly Sc)	$1.0 \leqslant Tauto$	75.0	45.9

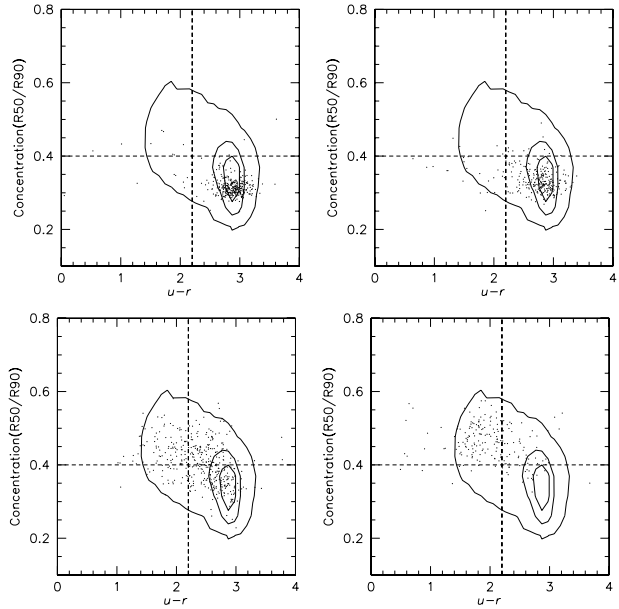

Figure 6. Cin is plotted against $u-r$. The contours show distribution of all galaxies in the volume limited sample. Points in each panel show the distribution of each morphological type of galaxies classified by eye (Shimasaku et al. 2001; Nakamura et al. 2003). Ellipticals are in the upper left panel. S0, Sa and Sc are in the upper right, lower left and lower right panel, respectively.

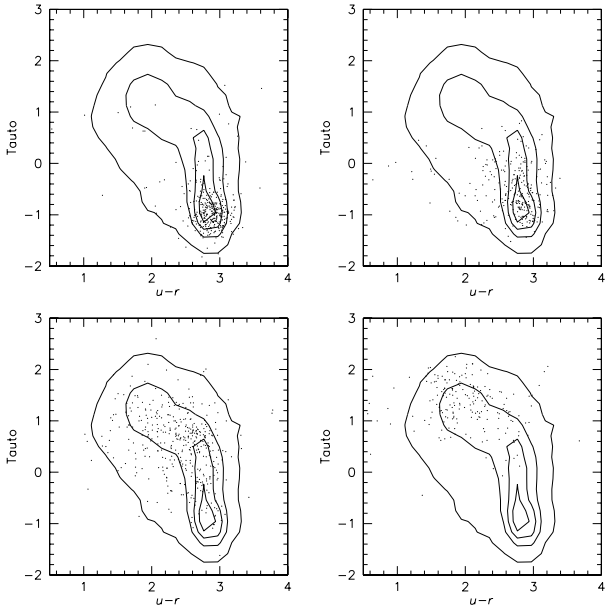

Figure 7. $Tauto$ is plotted against $u-r$. The extension of the distribution around $u-r$=2.8 is due to the inclination correction adopted in $Tauto$. The contours show distribution of all galaxies in the volume limited sample. Points in each panel show the distribution of each morphological type of galaxies classified by eye (Shimasaku et al. 2001; Nakamura et al. 2003). Ellipticals are in the upper left panel. S0, Sa and Sc are in the upper right, lower left and lower right panel, respectively.

from the uncertainty in background subtraction. In figure 10, we present distributions of this local galaxy density for all galaxies, galaxies within 0.5 Mpc from a cluster centre and galaxies between 1 and 2 Mpc from a cluster centre. In measuring distance form a cluster, we use the C4 cluster catalog (Miller et al. 2003). Part of the catalog is also presented in Gomez et al. (2003). For each galaxy, the distance from the nearest cluster centre is measured on a projected sky for galaxies within $\pm$1000 km s^{-1} from a cluster redshift.

4 RESULTS

4.1 The Morphology Density Relation in the SDSS Data

In figure 11, we use Cin to present the ratio of the number of early type galaxies to that of all galaxies as a function of the local galaxy density. The solid line shows the ratio of early type galaxies using Cin=0.4 as a separator, which separate elliptical galaxies and spiral galaxies well as shown in figure 6. The fraction of early type galaxies clearly increases with increasing density. In the least dense region, only 55% are early type, whereas in the densest region, almost 85% are early type galaxies. Furthermore, it is interesting to see that around galaxy density 3 Mpc^{-2}, the slope of the morphology-density relation abruptly becomes flatter. 3 Mpc^{-2} is a characteristic density for cluster perimeter (1-2 Mpc; see figure 10) and also coincides with the density where star formation rate (SFR) of galaxies changes as studied by Lewis et al. (2002) and Gomez et al. (2003). To see the dependence of the relation to the choice of our morphological criterion (Cin=0.4), we use slightly different criteria for dashed and dotted lines, which use Cin=0.37 and Cin=0.43 as a criterion, respectively. The former criterion is a little biased to spiral galaxies and the latter to elliptical galaxies. As is seen in the figure, both dotted and dashed lines show the morphology-density relation, but in somewhat flatter way than the solid line, indicating the effect of the contamination from spiral galaxies in case of Cin=0.43 (incompleteness in case of Cin=0.37). In the density below 3 Mpc^{-2}, the steepness of three slopes are almost identical.

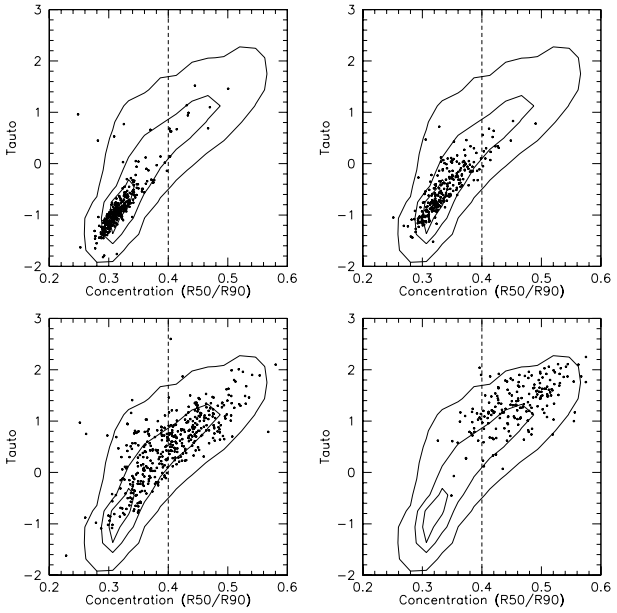

Figure 8. *Tauto* is plotted against *Cin*. The contours show distribution of all galaxies in the volume limited sample. A good correlation between two parameters is seen. The extension of the distribution to the upper left panel is due to the inclination correction of *Tauto*. Points in each panel show the distribution of each morphological type of galaxies classified by eye (Shimasaku et al. 2001; Nakamura et al. 2003). Ellipticals are in the upper left panel. S0, Sa and Sc are in the upper right, lower left and lower right panel, respectively.

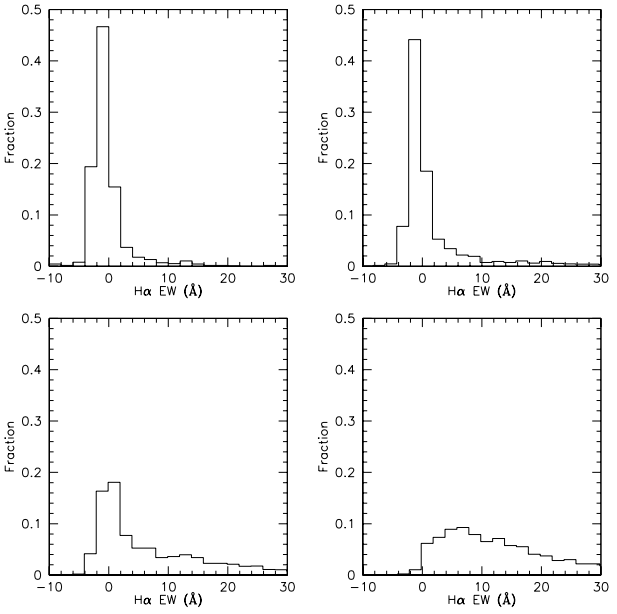

Figure 9. Distribution of Hα EW for four types classified with *Tauto*. A line in each panel shows the distribution of each morphological type of galaxies classified by *Tauto*. Early-type galaxies are in the upper left corner. Intermediate-type, early-disc and late-disc galaxies are in the upper right, lower left and lower right panel, respectively. An increase of Hα EW toward later type galaxies suggests that our morphological classification works well.

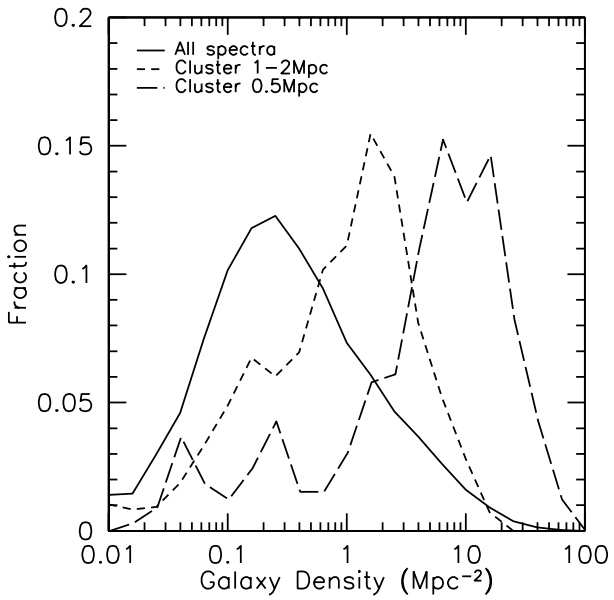

Figure 10. Distribution of local galaxy density. The solid, dashed and dotted lines show distributions for all galaxies, galaxies within 0.5 Mpc from the nearest cluster and galaxies between 1 and 2 Mpc from the nearest cluster, respectively.

However, at the densest region, only 65% is early-type galaxies in case of *Cin*=0.37, whereas almost 90% is early-type galaxies in case of *Cin*=0.43. Thus, the absolute amount of early-type galaxies are strong function of *Cin* criterion. Therefore, careful attention to *Cin* criterion is needed when comparing to other work such as computer simulations and other observational data.

In figure 12, the ratio of four morphological types of galaxies are plotted against galaxy density using *Tauto*. The short-dashed, solid, dotted and long-dashed lines represent early-type (E), intermediate (I), early-disc (ED) and late-disc (LD) galaxies, respectively. The error bars are calculated using Poisson statistics. The histogram in the upper panel shows the numbers of galaxies in each bin of the local galaxy density. The decline of late-disc fraction in going toward high density is seen. Early-disc fractions stays almost constant. Intermediate-type fractions dramatically increase toward higher density, but declines somewhat at the two highest density bins. Early-type fractions show mild increase with increasing density and radically increase at the two highest density bins. In the figure, there exist two characteristic densities where the relation radically changes. Around galaxy density 1 Mpc $^{-2}$, corresponding to the cluster infalling region (Fig. 10), the slope for late-disc suddenly goes down and the slope for intermediate-type rises up. At around galaxy density 6 Mpc $^{-2}$, corresponding to the cluster core region (Fig. 10), intermediate-type fractions suddenly goes down and early-type fractions show a sudden increase. To clarify this second change in early-type and intermediate-type fractions, we plot intermediate-type to early-type number ratio against local galaxy density in figure 13. As is seen in the previous figure, I/E ratio mildly increases from galaxy density 1 to 5 Mpc $^{-2}$, then suddenly declines after 6 Mpc $^{-2}$. We discuss the interpretation of this result in Section 5. The current results are derived from only ∼5% of the final

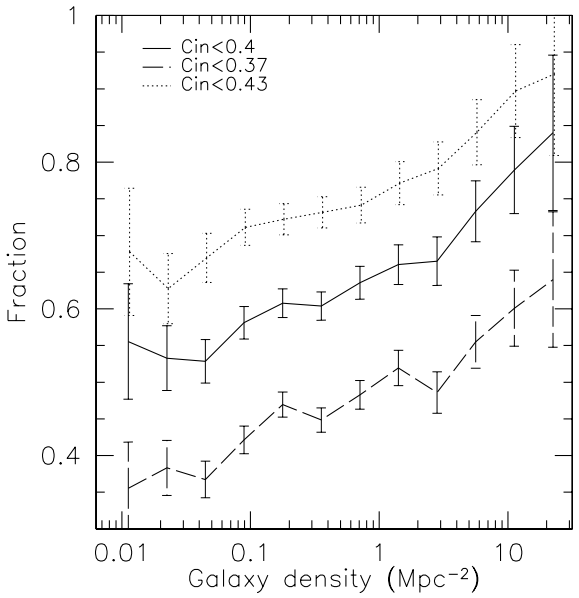

Figure 11. The morphology-density relation for three criteria of *Cin*. Fractions of early-type galaxies are plotted against local galaxy density. Three criteria are *Cin* <0.4, *Cin* <0.43 and *Cin* <0.37 in the solid, dashed and dotted lines, respectively. We do not include galaxy density >30 Mpc^{-2} in this plot since above this density there are only a few galaxies in each bin.

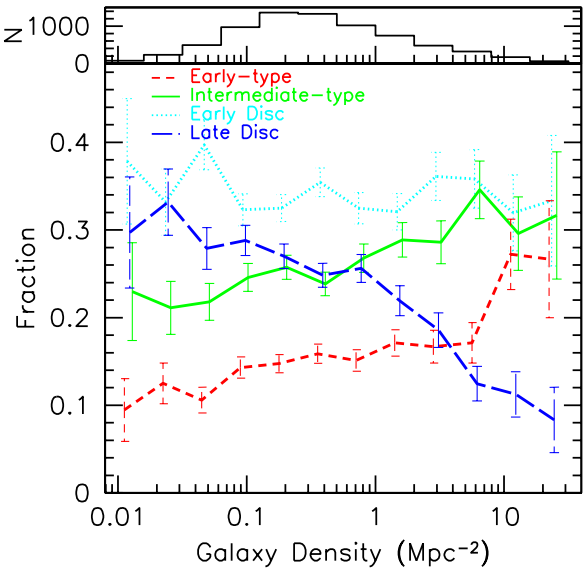

Figure 12. The morphology-density relation for four types of galaxies classified with *Tauto*. The short-dashed, solid, dotted and long-dashed lines represent early-type, intermediate-type, early-disc and late-disc galaxies, respectively. The histogram in the upper panel shows the numbers of galaxies in each bin of local galaxy density.

SDSS data. When the SDSS is completed, the errors on each data point will be reduced by approximately 80%.

4.2 Morphology-Radius Relation in the SDSS Data

In figure 14, we plot early-type fractions classified with *Cin*, against a radius from the cluster centre. We use the C4 galaxy cluster catalog (Miller et al. 2003) when measuring the distance between a galaxy and the nearest cluster. For each cluster, distances are measured by converting angular separation into physical distance for galaxies within ±1000 km s^{-1} in redshift space. For each galaxy, the distance to the nearest cluster is adopted as a distance to a cluster. The distance is converted to in a unit of one virial radius using velocity dispersion given in Miller et al. (2003) and the equation given in Girardi et al. (1998). The morphological fraction for each radius bin is measured in the same way as the last section; the solid, dashed and dotted lines represents different criteria, *Cin* =0.4, 0.37 and 0.43, respectively. As seen in figure 6, *Cin* =0.4 best separates elliptical and spiral galaxies. In the figure, fraction of early-type galaxies decreases toward larger distance from a cluster centre. The relation becomes consistent with flat after 1 virial radius. As in the case in figure 11, three criteria show similar slope. However, absolute amount of early-type galaxies is a strong function of *Cin* criteria. In case of *Cin*=0.4, early-type fractions increase from 60% to almost 90% toward a cluster centre.

In figure 15, we plot the morphology–cluster-centric-radius relation for four types of galaxies classified using *Tauto*. As is in figure 12, the short-dashed, solid, dotted

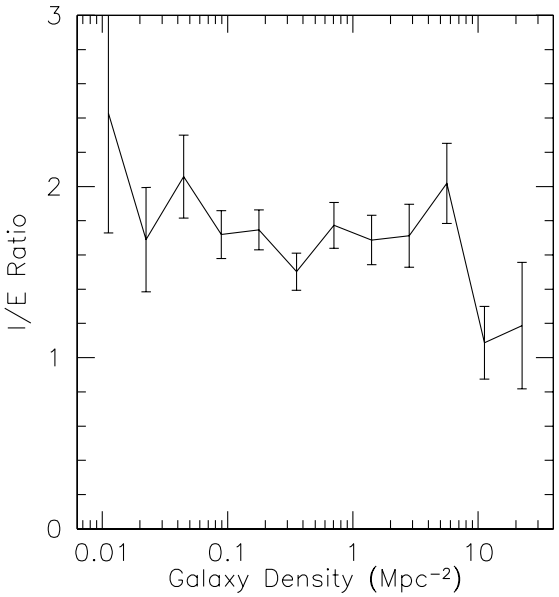

Figure 13. Intermediate-type to early-type number ratio as a function of local galaxy density.

and long-dashed lines represent early-type, intermediate-type, early-disc and late-disc galaxies, respectively. The error bars are calculated using Poisson statistics. The histogram in the upper panel shows the numbers of galaxies in each bin of cluster-centric radius. Fractions of late-disc galaxies decrease toward smaller radius, whereas fractions of early-type and intermediate galaxies increase toward a

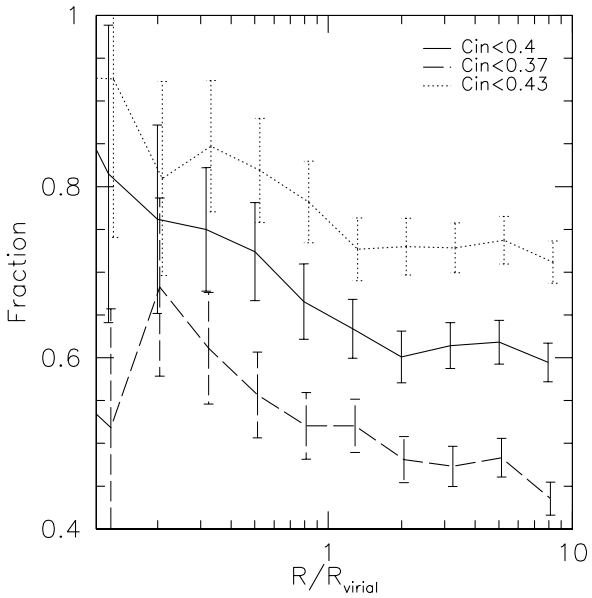

Figure 14. The morphology-radius relation based on *Cin*. Fractions of early-type galaxies are plotted against cluster-centric radius to the nearest cluster. Morphological criteria are *Cin* <0.4, *Cin* <0.43 and *Cin* <0.37 in the solid, dashed and dotted lines, respectively.

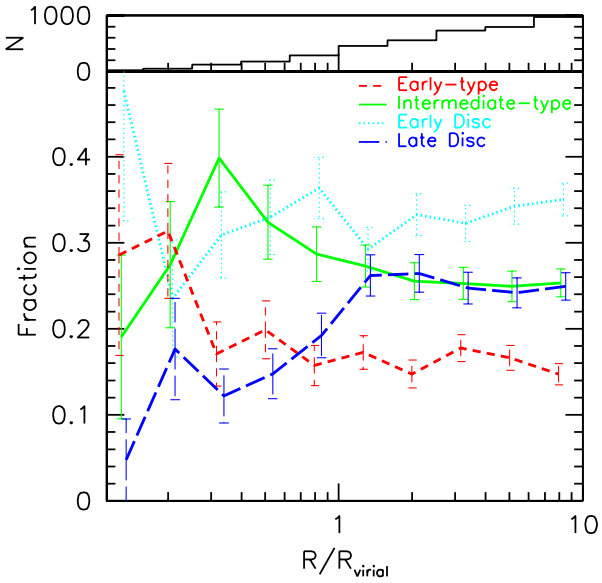

Figure 15. The morphology-radius relation based on *Tauto*. Fractions of each type of a galaxy is plotted against cluster-centric radius to the nearest cluster. The short-dashed, solid, dotted and long-dashed lines represent early-type, intermediate-type, early-disc and late-disc galaxies, respectively. The histogram in the upper panel shows the numbers of galaxies in each bin of cluster-centric radius.

cluster centre. In the figure, three characteristic radii are found. Above 1 virial radii, four lines are consistent with flat, suggesting that physical mechanisms responsible morphological change do not work beyond this radius. Between 0.3 and 1 virial radius, intermediate-type fractions mainly increases toward a cluster centre. Late- and early-disc galaxies show corresponding decrease. Interestingly intermediate-type fractions increase more than early-type fractions. Below 0.3 virial radius, early-type fractions dramatically increase and intermediate-type fractions decrease in turn. To further clarify the change between intermediate-type and early-type fractions, we plot intermediate to early-type number ratio in figure 16. As is seen in the figure 13, the ratio slightly increase between 1 and 0.3 virial radius toward a cluster centre. At 0.3 virial radius, slope changes radically and the ratio decreases toward a cluster centre. We interpret these findings in Section 5.

4.3 Density vs. Radius

To investigate the assertion that the morphology–cluster-centric-radius relation is more fundamental than the morphology–density relation (Whitmore et al. 1993), we divide the morphology-density relation at $R_{vir} = 1$, and plot it in Figure 17. The upper left, upper right, lower left and lower right panels represent early-type, intermediate-type, early disc and late disc galaxies, respectively. In each panel, the solid lines use galaxies with $R_{vir} < 1$ and the dashed lines use galaxies with $R_{vir} \geqslant 1$. In the figure, there is no significant difference in the fractions of early-type, early disc and late disc galaxies between inside and outside of $R_{vir} = 1$. However, even at low galaxy density ($< 1\mathrm{Mpc}^{-2}$) a huge excess of intermediate-type galaxies can be seen in the fractions of intermediate-type galaxies with $R_{vir} < 1$. The existence of the large fraction of intermediate-type galaxies at low galaxy density regions inside of $R_{vir} = 1$ suggest that intermediate-type galaxies can be created even at low density regions inside a cluster, and that the cluster environment is more fundamental than local galaxy density in creating intermediate-type galaxies. It should be noted that

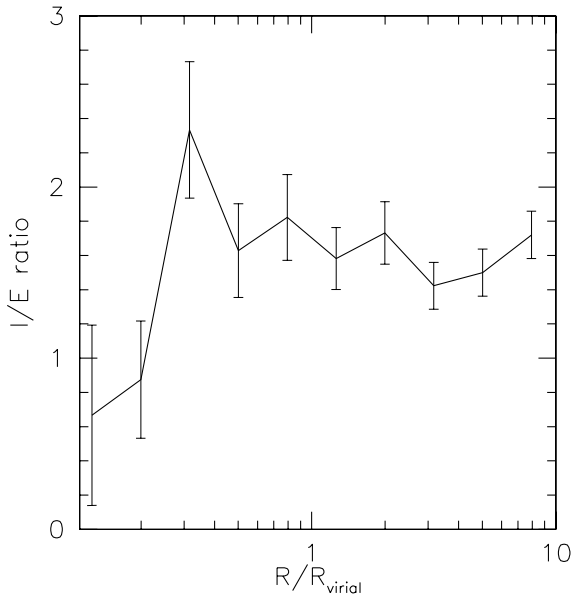

Figure 16. Intermediate-type to early-type number ratio is plotted against cluster centric radius. The ratio decreases at the cluster core region.

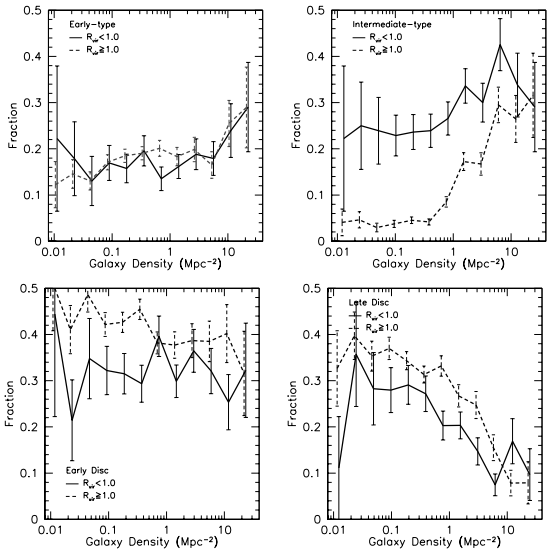

Figure 17. The morphology-density relation divided by $R_{vir} = 1$. The solid lines represent galaxies with $R_{vir} < 1$. The dashed lines represent galaxies with $R_{vir} \geqslant 1$. Early-types are in the upper left panel. Intermediate-types, early discs and late discs are in the upper right, lower left and lower right panel, respectively.

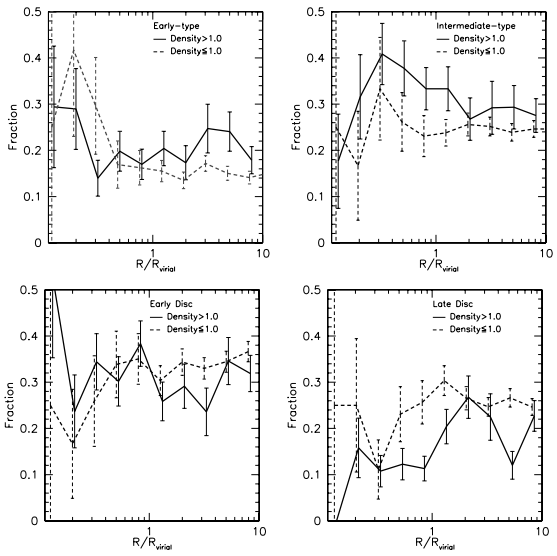

Figure 18. The morphology–cluster-centric-radius relation divided at the local galaxy density = 1 Mpc^{-2}. The solid lines represent galaxies with local galaxy density> 1. The dashed lines represent galaxies with local galaxy density≤ 1. Early-types are in the upper left panel. Intermediate-types, early discs and late discs are in the upper right, lower left and lower right panel, respectively.

Dominguez et al. (2001) performed a similar analysis in their Figures 7 and 8. However, they did not find the difference in elliptical+S0 fractions between small cluster-centric radius and large cluster-centric radius with low local galaxy density as we found in Figure 17. One possible explanation to this apparent discrepancy is that Dominguez et al. (2001) did not separate elliptical and S0 galaxies morphologically. It would be interesting to investigate whether their sample shows similar results with ours when elliptical and S0 galaxies are separated. In Figure 18, we plot the morphology–cluster-centric-radius relation divided by the local galaxy density at 1 Mpc^{-2}. The panels and symbols are same as in Figure 17. Since the local galaxy density and the cluster-centric-radius correlates themselves, it is difficult to see whether one is more fundamental than the other in this figure. However, in the upper right panel, intermediate-type fractions increase toward small cluster-centric-radius in both high and low local galaxy density regions, supporting our finding in Figure 17.

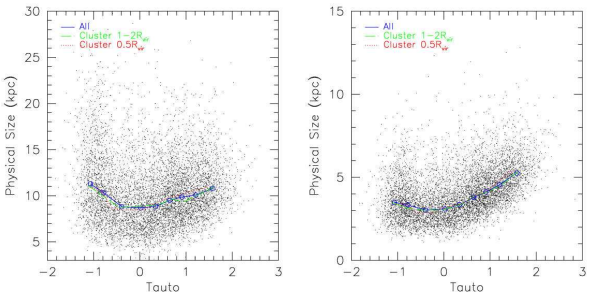

Figure 19. Physical sizes of all galaxies in the volume limited sample are plotted against $Tauto$ with the small dots. Petrosian 90% and 50% flux radius in r band is used to calculate physical sizes of galaxies in the left and right panel, respectively. The solid, dashed and dotted lines show medians of all galaxies, galaxies with 1< R_{vir} <2 and galaxies with R_{vir} <0.5 in the volume limited sample, respectively. In both panels, the medians turn over around $Tauto$ ∼0, corresponding to S0 population.

4.4 Physical Sizes of Galaxies

It is important to understand relative galaxy sizes when we discuss transformation of galaxies. In the left panel of figure 19, we plot physical galaxy sizes calculated using Petrosian 90% flux radius in r band, against $Tauto$ for all galaxies in the volume limited sample in the small dots. The solid, dashed and dotted lines show medians of all galaxies, galaxies with 1< R_{vir} <2 and galaxies with R_{vir} <0.5 in the volume limited sample, respectively. All the three lines show a consistent trend, suggesting that our $Tauto$ parameter is not affected by the specific environment of galaxies. Above $Tauto$=0, galaxy sizes decrease with decreasing $Tauto$. However, below $Tauto$=0, galaxy sizes increase with decreasing $Tauto$. The same trend can be found in the right panel of figure 19 where we used Petrosian 50% flux radius to perform the same analysis. We discuss the result in conjunction with Figs. 12 and 15 in Section 5.

4.5 Comparison with the MORPHS Data

In this section, we compare the morphology-density relation of the SDSS data (z ∼0.05) with that of the MORPHS data (z ∼0.5). The MORPHS data are used in Dressler et al. (1997) to study the morphology-density relation in high redshift clusters, and publicly available in Smail et al. (1997). The data consist of 10 rich galaxy clusters at a redshift range z =0.37-0.55 as summarized in table 2. The sharp imaging ability of the Hubble Space Telescope made it possible to

Table 2. THE MORPHS CLUSTER SAMPLE

Name	R.A.	Dec.	z	filter	$L_{X\ 0.3-3.5keV}(10^{43}h^{-2}$ ergs $s^{-1})$	σ (km s^{-1})
A370#2	02 40 01.1	−01 36 45	0.37	F814W	2.73	1350 [34]
Cl1447+23	14 49 28.2	+26 07 57	0.37	F702W	...	...
Cl0024+16	00 26 35.6	+17 09 43	0.39	F814W	0.55	1339 [33]
Cl0939+47	09 43 02.6	+46 58 57	0.41	F814W	1.05	1081 [31]
Cl0939+47#2	09 43 02.5	+46 56 07	0.41	F814W	1.05	1081[31]
Cl0303+17	03 06 15.9	+17 19 17	0.42	F702W	1.05	1079 [21]
3C295	14 11 19.5	+52 12 21	0.46	F702W	3.20	1670 [21]
Cl0412−65	04 12 51.7	−65 50 17	0.51	F814W	0.08	...
Cl1601+42	16 03 10.6	+42 45 35	0.54	F702W	0.35	1166 [27]
Cl0016+16	00 18 33.6	+16 25 46	0.55	F814W	5.88	1703 [30]
Cl0054−27	00 56 54.6	−27 40 31	0.56	F814W	0.25	...

measure galaxy morphology at this further away in the universe. We use concentration parameter given in Smail et al. (1997) as an automated morphology of the sample. It is more interesting to apply the $Tauto$ parameter to the MORPHS data. However, any morphological parameter needs careful calibration between high and low redshift imaging data where a pixel size and a psf size compared with a galaxy size are very different. We found such calibration is easier and more trustable for a concentration parameter as is used below. As for the galaxy density, we count a number of galaxies brighter than $Mr^* = -19.0$ within 250 kpc and subtracted average galaxy number count of the area (Glazebrook et al. 1995). Magnitude (either F702W or F814W) are k-corrected and transformed to the SDSS r band using the relation given in Fukugita et al. (1995). To make as fair comparison as possible, we re-measured the SDSS morphology-density relation using as similar criteria as possible. We re-measure galaxy density by counting galaxies within 250 kpc and ±1000 km s^{-1} and brighter than $Mr^* = -19.0$ in the SDSS data ($0.01< z <0.054$). The number of galaxies is divided by the size of the area ($250^2\ \pi$ kpc^2 if it does not go outside of the boundary. If it does, the area is corrected accordingly.) We also match the criteria for both of concentration parameters. The concentration parameter of the SDSS is measured as a ratio of Petrosian 50% light radius to 90% light radius. The concentration parameter of the MORPHS data is measured using the Source Extractor. Furthermore, the seeing size compared with typical galaxy size is not exactly the same between two samples. Therefore, we have to calibrate these two concentration parameters. Fortunately part of the SDSS galaxies are morphologically classified by eye in Dressler (1980). Since the MORPHS data are eye-classified by the same authors (Dressler et al. 1997), we regard these two eye-classified morphology essentially the same and use them to calibrate two concentration parameters. If we use the SDSS concentration criteria, Cin <0.4, It leaves 76% of eye-classified elliptical galaxies (24% contamination). By adjusting concentration parameter for the MORPHS data to this value, we found that the MORPHS concentration parameter of 0.45 leaves 75% of eye-classified elliptical galaxies. We regard these essentially the same criteria and adopt 0.45 as a criteria for the MORPHS concentration parameter which corresponds to that of the SDSS(Cin=0.4). In figure 20, we plot fractions of early-type galaxies against galaxy density for both the SDSS and MORPHS data in the solid and dashed lines, respectively. Quite interestingly, two morphology-density relations lie on top of each other. Since the MORPHS data only exist for cluster region, we are not able to probe into as low density regions as in figure 12. However, it shows that the morphology-density relation was already established at $z \sim 0.5$. There is a sign of slight excess of early-type galaxies in the SDSS data in two highest density bins.

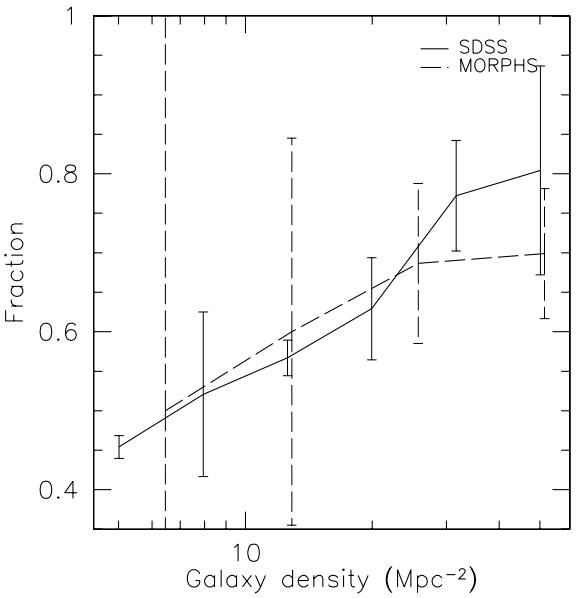

Figure 20. Comparison of the morphology-density relations of the SDSS (low redshift) and the MORPHS (high redshift). Fraction of early-type galaxies are plotted against local galaxy density within 250 kpc (Note that the local galaxy density here is measured in a different way from that in previous sections). The MORPHS data are plotted in the solid line, and the SDSS data are plotted in the dashed line.

5 DISCUSSION

5.1 Early-type Fractions

In previous section, we have presented fractions of early-type galaxies in several different ways. Since our morpho-

logical classification, density measurement are different from most of previous work, it is important to know how these early-type fractions differ due to the choice of relevant parameters. We use the result of Whitmore et al. (1993) as a benchmark for our study since they applied various systematic corrections carefully and the results are relatively widely used. Their fraction ratio of galaxies is elliptical:S0:spiral=18%:23%:59%. In figure 11, we have 55% of early-type galaxies in the least dense bin and 85% of them in the densest bin. In figure 14, our early-type fractions vary from 60% to 90%. Between these two figures, our values agree each other within the errors, suggesting our values are internally consistent. However, our early-type fractions are slightly lower than the sum of ellipticals and S0s (41%) in Whitmore et al. (1993). As noted in section 3, this comes from our choice of Cin=0.4 criteria slightly leaned toward spiral galaxies. Figure 11 showed that slight change in Cin criteria can change absolute amount of early-type galaxies dramatically, and thus, careful attention is needed when comparing our work with others. In our case, Cin=0.37 criteria shown in dotted line in figure 11 is closer to the classification of Whitmore et al. (1993).

In figure 12, we have 10% of early-type in the least dense bin and 25% in the densest bin. Intermediate-type galaxies are 25% in the least dense bin. In figure 15, early-type fractions vary from 15% to 30% and intermediate-type fractions vary from 25% to 40%. Again our values are consistent within the errors internally. In addition, in these cases, values are only two sigma away from Whitmore et al. (1993). If we add early-type fractions and intermediate-type fractions, our values are 30% and 35%, whereas Whitmore reports 41%. Therefore, in case of $Tauto$ parameter, our choice of criteria is similar to that of Whitmore et al. (1993).

5.2 The Morphology-Density Relation with Cin

In section 4.1, two interesting results are found in the SDSS data using Cin=0.4 as a classification criterion; (i) the morphology-density relation exists in the SDSS data, however it flatters out at low density. (ii) the characteristic galaxy density is at around 3 Mpc^{-2}. In section 4.2, we analyzed the morphology-density relation in the view point of the morphology-radius relation. The flattering at low density is seen as well with its turning point at around 1 R_{vir}. Since computer simulations sometimes use different magnitude range, different density measurement and different morphological classification (often bulge-to-disc ratio), it is difficult to do accurate direct comparison. However, both of morphology-density relation and morphology-radius relation are qualitatively in agreement with computer simulations such as Okamoto et al. (2001), Diaferio et al. (2001), Springel et al. (2001) and Benson et al. (2001). The flattering of morphology-density relation we saw in both figures 11 and 14 is interesting since it suggests that whatever physical mechanism is responsible for morphological change of late-disc galaxies in going toward dense regions, the mechanism starts working at galaxy density $\sim$3 Mpc^{-2} or higher.

Various mechanism can be responsible for the morphological change. These include ram-pressure stripping of gas (Spitzer & Baade 1951; Gunn & Gott 1972; Farouki & Shapiro 1980; Kent 1981; Abadi, Moore & Bower 1999; Fujita & Nagashima 1999; Quilis, Moore & Bower 2000), galaxy harassment (Moore et al. 1996, 1999; Fujita 1998), cluster tidal forces (Byrd & Valtonen 1990; Valluri 1993; Fujita 1998), enhanced star formation (Dressler & Gunn 1992), and removal & consumption of the gas (Larson, Tinsley & Caldwell 1980; Bekki et al. 2002). It is yet unknown exactly what processes play major roles in creating morphology-density relation. However, the mechanism must be the one that works at galaxy density 3 Mpc^{-2} or higher. It is also interesting to note that this characteristic density coincides with the density where galaxy SFR abruptly drops (Lewis et al. 2002; Gomez et al. 2003). The coincidence suggests that the same mechanism might be responsible for both morphology-density relation and the truncation of star formation.

5.3 The Morphology-Density Relation with $Tauto$

In figures 12 and 15, we further studied the morphology-density and the morphology-radius relation using $Tauto$ parameter, which allows us to divide galaxies into four categories (early, intermediate, early-disc and late-disc). In addition to the general trend found in the previous section, we found two characteristic changes in the relation at around galaxy density 1 and 6 Mpc^{-2} or in terms of radius, 0.3 and 1 virial radii. In the sparsest regions (below 1 Mpc^{-2} or outside of 1 virial radius), both relations becomes almost flat, suggesting the responsible physical mechanisms do not work very well in these regions. In the intermediate regions (density between 1 and 6 Mpc^{-2} or virial radius between 0.3 and 1), intermediate-type fractions dramatically increase toward denser or smaller radius regions, whereas fractions of late-disc galaxies decrease. In the densest regions (above 6 Mpc^{-2} or inside of 0.3 virial radius), interestingly intermediate-type fractions decrease, and in turn, early-type fractions radically increase suddenly. The change in the densest region are further confirmed in figures 13 and 16, where we plotted intermediate to early-type number ratio as a function of density or cluster-centric-radius. In both figures, intermediate to early-type ratio declines suddenly at the densest region.

The existence of two characteristic change in both the morphology-density and the morphology-radius relation suggests the existence of two different physical mechanisms responsible for each morphological fraction change. In the intermediate region (density between 1 and 6 Mpc^{-2} or virial radius between 0.3 and 1), the mechanism creates intermediate-type galaxies mostly, by reducing fractions of late-disc galaxies. Although there is not much change in early-disc fractions, perhaps it is natural to imagine that the mechanism turns late-disc galaxies into early-disc galaxies, and then early-disc galaxies into intermediate-type galaxies. As figure 19 shows, median sizes of galaxies gradually declines from late-discs to intermediate-type galaxies, suggesting calm, gradual transformation of galaxies, maybe due to the truncation of star formation as observed at the same environment by Gomez et al. (2003) and Lewis et al. (2002). After the truncation of star formation, outer part of a galaxy disc fades away as massive stars die. In fact, such a galaxy in transition is found by Goto et al. (2003a), who showed that spiral galaxies with no emission lines (passive spirals) preferentially live in cluster infalling regions. The calm, quiescent truncation of the star formation is also supported by our

findings in Section 4.3, where we found that intermediate-type galaxies can be created inside of $R_{vir} = 1$ regardless of the local galaxy density. The results imply that cluster environment such as interaction with hot, plasma gas associated with cluster potential is more important to create intermediate-type galaxies than the process induced by the enhancement of local galaxy density (e.g., galaxy-galaxy merger/interaction). The plausible candidates of the responsible mechanism includes ram-pressure stripping (Gunn & Gott 1972; Farouki & Shapiro 1980; Kent 1981; Fujita & Nagashima 1999; Abadi, Moore & Bower 1999; Quilis, Moore & Bower 2000; Fujita 2001, 2003), unequal mass galaxy mergers (Bekki et al. 1998), galaxy harassment (Moore et al. 1999) and truncation of star formation due to the cluster environment (strangulation; Larson, Tinsley & Caldwell 1980; Bekki et al. 2002; Mo & Mao 2002; Oh & Benson 2001), evaporation of the cold gas in disc galaxies via heat conduction from the surrounding hot ICM (Cowie & Songaila 1977; Fujita 2003). Although several authors indicated that these regions are too low gas density for stripping to happen (e.g., Lewis et al. 2002), Fujita (2003) pointed out that ram-pressure stripping may be effective in cluster sub-clump regions. In fact, Kodama et al. (2001) found galaxy colours suddenly change in such sub-clump regions. Perhaps, it is also worth noting that E+A (K+A or post-starburst) galaxies often thought to be cluster-related are found to have their origin in merger/interaction with accompanying galaxies (Goto et al. 2003b,c), and thus E+A galaxies are not likely to be a product of the morphological transition in these cluster regions.

Very different consequences are found in the densest region (above 6 Mpc^{-2} or inside of 0.3 virial radius), where the mechanism decrease intermediate-type fractions and increase early-type fractions. In figure 19, there is a significant increase in median galaxy sizes from intermediate-type to early-type galaxies. Both of these observational results suggest a very different mechanism from intermediate region is working in the densest region. Since galaxy size becomes larger from intermediate-type to early-type galaxies (Figure 19), merging scenario is one of the candidate mechanisms. Computer simulations based on the galaxy merging scenario reported the deficit of intermediate-type galaxies (Okamoto et al. 2001; Diaferio et al. 2001; Springel et al. 2001; Benson et al. 2001), which we might have seen observationally in the densest region of our data. However, theoretical work in the literature suggests that merging/interaction is difficult to happen in cluster core regions since relative velocity of galaxies are too high in such regions (Ostriker 1980; Binney & Tremaine 1987; Mamon 1992; Makino & Hut 1997; but see also Mihos 2003). If this is the case, dominance of old early-type galaxies in cluster cores might be so extreme that early-type fractions overwhelm the increase of intermediate-type fractions in cluster cores. In previous work, Postman & Geller (1984) pointed out that their morphology-density relation has two breaks. Dominguez et al. (2002) suggested that there are two mechanisms in the morphology-density relation; one with global nature and the other with local effects. Our findings of two characteristic changes in the morphology-density relation is perhaps an observational result of the same physical phenomena as these from a different point of view.

5.4 Comparison with the MORPHS Data

In section 4.5, we compared the local morphology-density relation (SDSS; z $\sim$0.05) with that of higher redshift (MORPHS; 0.37$<$ z $<$0.5). Interestingly, two morphology-density relations agreed each other. The agreement suggests that morphology-density relation was already established at z $\sim$0.5 as it is in the present universe, i.e., the origin of morphology-density relation stays much higher redshift universe. In the densest environments, there might be a sign of excess early-type fractions in the SDSS than in the MORPHS. Although two data points agrees within the error, such an excess of early-type galaxies might suggest additional formation of elliptical/S0 galaxies between z =0.5 and z =0.05. If it is the case, the result may be consistent with Dressler et al. (1997) and Fasano et al. (2000), where they observed the increase of S0 galaxies toward lower redshift and proposed spiral to S0 transformation. Little evolution of morphology-density relation is also interesting in terms of comparison with computer simulations. Benson et al. (2001) predicted that the evolution of morphology-density relation will be seen as a shift in the decrease of early-type fractions without significant change in slope.

However, a caveat is that absolute value in Figure 20 depends solely on the calibration of concentration parameters of the both data, which by nature is difficult to calibrate accurately due to the large scatter in both concentration parameters. Therefore, the results on evolution should not be over-interpreted. In addition, the richness of the MORPHS clusters and the SDSS clusters are very different. The MORPHS sample consists of rich clusters with their velocity dispersion $>$ 1000 km s^{-1} (Table 2), whereas the median velocity dispersion of the SDSS clusters is $\sim$700 km s^{-1} (Table 1 of Gomez et al. 2003). Since it is often reported that rich clusters might have fewer amount of blue/late-type galaxies than poor clusters (Margoniner et al. 2001; Goto et al. 2003d), it is more ideal to use clusters with similar richness for both high and low redshift samples. Such a study will become possible in the near future as the SDSS observes larger volume to find many rich clusters.

6 CONCLUSIONS

We have studied the morphology-density relation and the morphology–cluster-centric-radius relation using a volume limited sample of the SDSS data (0.05$<$ z $<$0.1, $Mr^* <$ $-$20.5). Compared with previous studies, major improvements in this work are; (i) automated galaxy morphology, (ii) three dimensional local galaxy density estimation, (iii) the extension of the morphology-density relation into the field region. Our findings can be summarized as follows.

Both the morphology-density relation and the morphology–cluster-centric-radius relation are seen in the SDSS data for both of our automated morphological classifiers, Cin and $Tauto$.

We found there are two characteristic changes in both the morphology-density and the morphology-radius relations, suggesting two different mechanisms are responsible for the relations. In the sparsest regions (below 1 Mpc^{-2} or outside of 1 virial radius), both relations become less effective, suggesting the responsible physical mechanisms re-

quire denser environment. The characteristic density or radius coincides with the sharp turn in SFR-density relation (Lewis et al. 2002; Gomez et al. 2003), suggesting the same mechanism might be responsible for both the morphology-density relation and SFR-density relation. In the intermediate density regions, (density between 1 and 6 Mpc^{-2} or virial radius between 0.3 and 1), intermediate-type fractions increase toward denser regions, whereas late-disc fractions decrease. Considering the median size of intermediate-type galaxies are smaller than that of late-disc galaxies (figure 19) and SFR radically declines in these regions, the mechanism that gradually reduces star formation might be responsible for morphological changes in these intermediate density regions (e.g., ram-pressure stripping). Quiescent truncation of star formation is also supported by our findings in Section 4.3, where we found that intermediate-type galaxies can be created inside of $R_{vir} = 1$ regardless of the local galaxy density. The results imply that cluster environment such as interaction with plasma gas associated with cluster potential is more important to create intermediate-type galaxies than the process induced by the enhancement of local galaxy density (e.g., galaxy-galaxy merger/interaction). The mechanism is likely to stop star formation in late-disc galaxies, then late-disc galaxies becomes early-disc galaxies and eventually turns into smaller intermediate-type galaxies after their outer discs and spiral arms become invisible as stars die. In the densest regions (above 6 Mpc^{-2} or inside of 0.3 virial radius), intermediate-type fractions decreases radically and early-type fractions increase. This is a contrasting results to that in intermediate regions and it suggests that yet another mechanism is responsible for morphological change in these regions. Considering that elliptical galaxies can be observed in high redshift universe (e.g., van Dokkum et al. 2000), dominance of elliptical galaxies might be so extreme in cluster cores that early-type fractions overwhelm the increase of intermediate-type fractions.

We also compared our morphology-density relation from the SDSS (z ∼0.05) with that of the MORPHS data (z ∼0.5). Two relations lie on top of each other, suggesting that the morphology-density relation was already established at z ∼0.5 as is in the present universe. In the densest bin, a slight sign of excess elliptical/S0 fraction was seen in the SDSS data, which might be indicating the formation of additional elliptical/S0 galaxies between z =0.5 and z =0.05.

ACKNOWLEDGMENTS

We are grateful to Michael L. Balogh, Robert C. Nichol, Masami Ouchi, Masayuki Tanaka, Alex Finoguenov and Ann Zabludoff for useful discussions. We wish to express our gratitude to Takashi Okamoto, Naoyuki Tamura, Masahiro Nagashima for useful conversation. We thank the anonymous referee for many insightful comments. T. G. acknowledges financial support from the Japan Society for the Promotion of Science (JSPS) through JSPS Research Fellowships for Young Scientists.

The Sloan Digital Sky Survey (SDSS) is a joint project of The University of Chicago, Fermilab, the Institute for Advanced Study, the Japan Participation Group, the Johns Hopkins University, the Max-Planck-Institute for Astronomy, New Mexico State University, Princeton University, the United States Naval Observatory, and the University of Washington. Apache Point Observatory, site of the SDSS telescopes, is operated by the Astrophysical Research Consortium (ARC). Funding for the project has been provided by the Alfred aP. Sloan Foundation, the SDSS member institutions, the National Aeronautics and Space Administration, the National Science Foundation, the U. S. Department of Energy, Monbusho, and the Max Planck Society. The SDSS Web site is http://www.sdss.org/.

REFERENCES

Abraham, R. G. et al. 1996, ApJ, 471, 694
Annis J., Kent S., Castander F., et al., 1999, AAS, 31, 1391
Bekki K., Couch W. J., Shioya Y., 2002, ApJ, 577, 651
Bekki, K. 1998, ApJL, 502, L133
Benson, A. J., Frenk, C. S., Baugh, C. M., Cole, S., & Lacey, C. G. 2001, MNRAS, 327, 1041
Binney, J., & Tremaine, S. 1987, Galactic Dynamics (Princeton: Princeton Univ. Press)
Blanton M. R., Lin H., Lupton R. H., Maley F. M., Young N., Zehavi I., Loveday J., 2003a, AJ, 125, 2276
Blanton M. R., Brinkmann J., Csabai I., et al., 2003b, AJ, 125, 2348
Byrd, G. & Valtonen, M. 1990, ApJ, 350, 89
Cole, S., Lacey, C. G., Baugh, C. M., & Frenk, C. S. 2000, MNRAS, 319, 168
Cowie, L. L. & Songaila, A. 1977, nature, 266, 501
Diaferio, A., Kauffmann, G., Balogh, M. L., White, S. D. M., Schade, D., & Ellingson, E. 2001, MNRAS, 323, 999
Domínguez, M. J., Zandivarez, A. A., Martínez, H. J., Merchán, M. E., Muriel, H., & Lambas, D. G. 2002, MNRAS, 335, 825
Domínguez, M., Muriel, H. ;., & Lambas, D. G. 2001, AJ, 121, 1266
Dressler, A. 1980, ApJ, 236, 351
Dressler, A. & Gunn, J. E. 1992, ApJS, 78, 1
Eisenstein, D. J. et al. 2001, AJ, 122, 2267
Ellingson, E., Lin, H., Yee, H. K. C., & Carlberg, R. G. 2001, ApJ, 547, 609
Fabricant D., Franx M., van Dokkum P., 2000, ApJ, 539, 577
Fasano, G., Poggianti, B. M., Couch, W. J., Bettoni, D., Kjærgaard, P., & Moles, M. 2000, ApJ, 542, 673
Finoguenov, A., Briel, U.G., Henry, J.P., 2003a, submitted to A&A
Finoguenov, A., Pietsch, W., Aschenbach, B., Miniati, F., 2003b, submitted to A&A
Fukugita, M., Shimasaku, K., & Ichikawa, T. 1995, PASP, 107, 945
Fukugita, M., Ichikawa, T., Gunn, J. E., Doi, M., Shimasaku, K., & Schneider, D. P. 1996, AJ, 111, 1748.
Fujita, Y. 1998, ApJ, 509, 587
Fujita, Y. & Nagashima, M. 1999, ApJ, 516, 619
Fujita, Y. 2001, ApJ, 550, 612
Fujita, Y. 2003, submitted to ApJ
Girardi, M., Giuricin, G., Mardirossian, F., Mezzetti, M., & Boschin, W. 1998, ApJ, 505, 74

Glazebrook, K., Ellis, R., Santiago, B., & Griffiths, R. 1995, MNRAS, 275, L19
Gómez, P. L. et al. 2003, ApJ, 584, 210
Goto T., Okamura S., McKay T. A., et al., 2002a, PASJ, 54, 515
Goto T., Sekiguchi M., Nichol R. C., et al., 2002b, AJ, 123, 1807
Goto T., Okamura S., Yagi M., et al. 2003a, PASJ, 55, 739
Goto T., Nichol R. C., Okamura S., et al. 2003b, PASJ, 55, 771
Goto T. 2003c, PhD Thesis, The University of Tokyo, astro-ph/0310196
Goto T., Okamura S., Sekiguchi M., et al. 2003d, PASJ, 55, 757
Gunn, J. E. & Gott, J. R. I. 1972, ApJ, 176,
Gunn J. E., Carr M., Rockosi C., et al., 1998, AJ, 116, 3040
Hashimoto, Y. & Oemler, A. J. 1999, ApJ, 510, 609
Helsdon S. F., Ponman T. J., 2003, MNRAS, 339, L29
Hogg D. W., Finkbeiner D. P., Schlegel D. J., Gunn J. E., 2001, AJ, 122, 2129
Hogg D. W., Blanton M. R., Eisenstein D. J., et al., 2003, ApJ, 585, L5
Icke, V. 1985, A&A, 144, 115
Kennicutt, R. C. 1998, ARAA, 36, 189
Kim R. S. J., Kepner J. V., Postman M., et al., 2002, AJ, 123, 20
Kodama, T. & Bower, R. G. 2001, MNRAS, 321, 18
Lahav, O. et al. 1995, Science, 267, 859
Larson, R. B., Tinsley, B. M., & Caldwell, C. N. 1980, ApJ, 237, 692
Lavery, R. J. & Henry, J. P. 1988, ApJ, 330, 596
Lewis, I. et al. 2002, MNRAS, 334, 673
Lupton R. H., Ivezic Z., Gunn J. E., Knapp G., Strauss M. A., Yasuda N., 2002, SPIE, 4836, 350
Lupton R. H., Gunn J. E., Ivezić Z., Knapp G. R., Kent S., Yasuda N., 2001, adass, 10, 269
Lupton R. H., Gunn J. E., Szalay A. S., 1999, AJ, 118, 1406
Makino, J. & Hut, P. 1997, ApJ, 481, 83
Mamon, G. A. 1992, ApJL, 401, L3
Margoniner V. E., de Carvalho R. R., Gal R. R., Djorgovski S. G., 2001, ApJ, 548, L143
Mihos, J.C. 2003, in Carnegie Observatories Astrophysics Series, Vol. 3: Clusters of Galaxies: Probes of Cosmological Structure and Galaxy Evolution, ed. J. S. Mulchaey, A. Dressler, & A. Oemler (Cambridge: Cambridge Univ. Press)
Miller, C. et al. in prep.
Mo, H. J. & Mao, S. 2002, MNRAS, 333, 768
Moore, B., Katz, N., Lake, G., Dressler, A., & Oemler, A. 1996, nature, 379, 613
Moore, B., Lake, G., Quinn, T., & Stadel, J. 1999, MNRAS, 304, 465
Nakamura O., Fukugita M., Yasuda N., Loveday J., Brinkmann J., Schneider D. P., Shimasaku K., SubbaRao M., 2003, AJ, 125, 1682
Oh S. P., Benson A. J., 2003, MNRAS, 342, 664
Okamoto, T. & Nagashima, M. 2001, ApJ, 547, 109
Ostriker, J. P. 1980, Comments on Astrophysics, 8, 177
Pier J. R., Munn J. A., Hindsley R. B., Hennessy G. S., Kent S. M., Lupton R. H., Ivezić Ž., 2003, AJ, 125, 1559
Postman M., Geller M. J., 1984, ApJ, 281, 95
Richards G. T., Fan X., Newberg H. J., et al., 2002, AJ, 123, 2945
Roberts M. S., Haynes M. P., 1994, ARA&A, 32, 115
Schlegel, D. J., Finkbeiner, D. P., & Davis, M. 1998, ApJ, 500, 525
Shectman, S. A., Landy, S. D., Oemler, A., Tucker, D. L., Lin, H., Kirshner, R. P., & Schechter, P. L. 1996, ApJ, 470, 172
Shimasaku, K. et al. 2001, AJ, 122, 1238
Shioya, Y., Bekki, K., Couch, W. J., & De Propris, R. 2002, ApJ, 565, 223
Smail, I., Dressler, A., Couch, W. J., Ellis, R. S., Oemler, A. J., Butcher, H., & Sharples, R. M. 1997, ApJS, 110, 213
Smith J. A., Tucker D. L., Kent S., et al., 2002, AJ, 123, 2121
Springel, V., White, S. D. M., Tormen, G., & Kauffmann, G. 2001, MNRAS, 328, 726
Stoughton, C. et al. 2002, AJ, 123, 485
Strateva, I. et al. 2001, AJ, 122, 1861
Strauss M. A., Weinberg D. H., Lupton R. H., et al., 2002, AJ, 124, 1810
Tran K. H., Simard L., Zabludoff A. I., Mulchaey J. S., 2001, ApJ, 549, 172
Treu T., Ellis R. S., Kneib J., Dressler A., Smail I., Czoske O., Oemler A., Natarajan P., 2003, ApJ, 591, 53
Whitmore B. C., Gilmore D. M., 1991, ApJ, 367, 64
Whitmore, B. C., Gilmore, D. M., & Jones, C. 1993, ApJ, 407, 489
Whitmore, B. C. 1995, ASP Conf. Ser. 70: Groups of Galaxies, 41
Valluri, M. 1993, ApJ, 408, 57
van Dokkum P. G., Franx M., Fabricant D., Illingworth G. D., Kelson D. D., 2000, ApJ, 541, 95
Yamauchi, C. et al. 2003, in prep.
Yee, H. K. C., Ellingson, E., & Carlberg, R. G. 1996, ApJS, 102, 269
York, D. G. et al. 2000, AJ, 120, 1579